

Autonomous observations of *in vivo* fluorescence and particle backscattering in an oceanic oxygen minimum zone

A. L. Whitmire,^{1,*} R. M. Letelier,¹ V. Villagrán,³ and O. Ulloa,²

¹College of Oceanic & Atmospheric Sciences, Oregon State University, Corvallis, OR 97330

²Departamento de Oceanografía and Centro de Investigación Oceanográfica (COPAS),
Universidad de Concepción, Concepción, Chile

³Departamento de Geofísica, Universidad de Concepción, Concepción, Chile

*whitmire@coas.oregonstate.edu

Abstract: The eastern South Pacific (ESP) oxygen minimum zone (OMZ) is a permanent hydrographic feature located directly off the coasts of northern Chile and Peru. The ESP OMZ reaches from coastal waters out to thousands of kilometers offshore, and can extend from the near surface to depths greater than 700 m. Oxygen minimum zones support unique microbial assemblages and play an important role in marine elemental cycles. We present results from two autonomous profiling floats that provide nine months of time-series data on temperature, salinity, dissolved oxygen, chlorophyll *a*, and particulate backscattering in the ESP OMZ. We observed consistently elevated backscattering signals within low-oxygen waters, which appear to be the result of enhanced microbial biomass in the OMZ intermediate waters. We also observed secondary chlorophyll *a* fluorescence maxima within low-oxygen waters when the upper limit of the OMZ penetrated the base of the photic zone. We suggest that autonomous profiling floats are useful tools for monitoring physical dynamics of OMZs and the microbial response to perturbations in these areas.

© 2009 Optical Society of America

OCIS codes: (010.4450) Oceanic Optics; (010.1350) Backscattering; (260.2510) Fluorescence; (290.5850) Scattering, particles

References and Links

1. R. Fuenzalida, W. Schneider, J. Garcés-Vargas, L. Bravo, and C. Lange, "Vertical and horizontal extension of the oxygen minimum zone in the eastern South Pacific Ocean," *Deep Sea Res. Part II Top. Stud. Oceanogr.* **56**(16), 992–1003 (2009) (doi:10.1016/j.dsr2.2008.11.001).
2. L. A. Codispoti, J. A. Brandes, J. P. Christensen, A. H. Devol, S. W. A. Naqvi, H. W. Paerl, and T. Yoshinari, "The oceanic fixed nitrogen and nitrous oxide budgets: Moving targets as we enter the anthropocene?" *Sci. Mar.* **65**(Suppl. 2), 85–105 (2001).
3. J. Karstensen, L. Stramma, and M. Visbeck, "Oxygen minimum zones in the eastern tropical Atlantic and Pacific oceans," *Prog. Oceanogr.* **77**(4), 331–350 (2008).
4. D. Kamykowski, and S.-J. Zentara, "Hypoxia in the world ocean as recorded in the historical data set," *Deep Sea Res. Part I Oceanogr. Res. Pap.* **37**(12), 1861–1874 (1990).
5. J. J. Helly, and L. A. Levin, "Global distribution of naturally occurring marine hypoxia on continental margins," *Deep Sea Res. Part I Oceanogr. Res. Pap.* **51**(9), 1159–1168 (2004).
6. L. Stramma, G. C. Johnson, J. Sprintall, and V. Mohrholz, "Expanding oxygen-minimum zones in the tropical oceans," *Science* **320**(5876), 655–658 (2008).
7. A. Paulmier, and D. Ruiz-Pino, "Oxygen minimum zones (OMZs) in the modern ocean," *Prog. Oceanogr.* **80**(3–4), 113–128 (2008) (doi:10.1016/j.pocean.2008.08.001).
8. A. Paulmier, D. Ruiz-Pino, V. Garçon, and L. Farias, "Maintaining of the Eastern south Pacific oxygen minimum zone (OMZ) off Chile," *Geophys. Res. Lett.* **33**(20), L20601 (2006).
9. V. Molina, L. Farías, Y. Eissler, L. A. Cuevas, C. E. Morales, and R. Escribano, "Ammonium cycling under the strong oxygen gradient associated with the Oxygen Minimum Zone off northern Chile (–23°S)," *Mar. Ecol. Prog. Ser.* **288**, 35–43 (2005) (doi: 10.3354/meps288035).

10. L. A. Cuevas, and C. E. Morales, "Nanoheterotroph grazing on bacteria and cyanobacteria in oxic and suboxic waters in coastal upwelling areas off northern Chile," *J. Plankton Res.* **28**(4), 385–397 (2006) (doi:10.1093/plankt/fbi124).
11. O. Ulloa, L. Belmar, L. Farias, M. Castro-Gonzalez, A. Galan, P. Lavin, V. Molina, S. Ramirez, F. Santibanez, and H. Stevens, "Microbial communities and their biogeochemical role in the water column of the oxygen minimum zone in the eastern South Pacific," *Gayana (Zool.)* **70**(1), 83–86 (2006).
12. R. Goericke, R. J. Olson, and A. Shalapyonok, "A novel niche for *Prochlorococcus* sp. in low-light suboxic environments in the Arabian Sea and the Eastern Tropical North Pacific," *Deep Sea Res. Part I Oceanogr. Res. Pap.* **47**(7), 1183–1205 (2000).
13. A. Galán, V. Molina, B. Thamdrup, D. Woebken, G. Lavik, M. M. M. Kuypers, and O. Ulloa, "Anammox bacteria and the anaerobic oxidation of ammonium in the oxygen minimum zone off northern Chile," *Deep Sea Res. Part II Top. Stud. Oceanogr.* **56**(16), 1021–1031 (2009) (doi: 10.1016/j.dsr2.2008.09.016).
14. H. Stevens, and O. Ulloa, "Bacterial diversity in the oxygen minimum zone of the eastern tropical South Pacific," *Environ. Microbiol.* **10**(5), 1244–1259 (2008) (doi:10.1111/j.1462-2920.2007.01539.x).
15. M. Castro-González, G. Braker, L. Farías, and O. Ulloa, "Communities of nirS-type denitrifiers in the water column of the oxygen minimum zone in the eastern South Pacific," *Environ. Microbiol.* **7**(9), 1298–1306 (2005).
16. H. Pak, L. A. Codispoti, and J. R. V. Zaneveld, "On the intermediate particle maxima associated with oxygen-poor water off Western South America," *Deep-Sea Res.* **27**(10), 783–797 (1980).
17. G. Kullenberg, "A comparison of distributions of suspended matter in the Peru and Northwest African upwelling areas," in *Coastal Upwelling*, F. A. Richards, ed., (American Geophysical Union 1982), pp. 282–290.
18. P. C. Garfield, T. Z. Packard, G. E. Friederich, and L. A. Codispoti, "A subsurface particle maximum layer and enhanced microbial activity in the secondary nitrite maximum of the northeastern tropical Pacific Ocean," *J. Mar. Res.* **41**(4), 747–768 (1983).
19. G. Kullenberg, "Observations of light scattering functions in two oceanic areas," *Deep-Sea Res.* **31**(3), 295–290 (1984).
20. A. M. Lewitus, and W. W. Broenkow, "Intermediate depth pigment maxima in oxygen minimum zones," *Deep-Sea Res.* **32**(9), 1101–1115 (1985).
21. R. W. Spinrad, H. Glover, B. B. Ward, L. A. Codispoti, and G. Kullenberg, "Suspended particle and bacterial maxima in Peruvian coastal waters during a cold water anomaly," *Deep-Sea Res.* **36**(5), 715–733 (1989).
22. S. W. A. Naqvi, M. D. Kumar, P. V. Narvekar, S. N. De Souza, M. D. George, and C. D'Silva, "An intermediate nepheloid layer associated with high microbial metabolic rates and denitrification in the Northwest Indian Ocean," *J. Geophys. Res.* **98**(C9), 16469–16479 (1993).
23. J. M. Morrison, L. A. Codispoti, S. L. Smith, K. Wishner, C. Flagg, W. D. Gardner, S. Gaurin, S. W. A. Naqvi, V. Manghnani, L. Prosperie, and J. S. Undersen, "The oxygen minimum zone in the Arabian Sea during 1995," *Deep Sea Res. Part II Top. Stud. Oceanogr.* **46**(8–9), 1903–1931 (1999).
24. T. Dickey, "The emergence of concurrent high resolution physical and bio-optical measurements in the upper ocean and their applications," *Rev. Geophys.* **29**(3), 383–413 (1991).
25. G. C. Chang, and T. D. Dickey, "Optical and physical variability on time scales from minutes to the seasonal cycle on the New England shelf: July 1996 - June 1997," *J. Geophys. Res.* **106**(C5), 9435–9453 (2001).
26. E. Boss, D. Stramski, T. Bergmann, W. S. Pegau, and M. Lewis, "Why should we measure the optical backscattering coefficient?" *Oceanography (Wash. D.C.)* **17**(2), 44–49 (2004).
27. E. Boss, M. J. Perry, D. Swift, L. Taylor, P. Brickley, J. R. V. Zaneveld, and S. Riser, "Three Years of Ocean Data From a Bio-optical Profiling Float," *Eos Trans. AGU* **89**(23), 209–210 (2008).
28. E. Boss, D. Swift, L. Taylor, P. Brickley, J. R. Zaneveld, S. Riser, M. J. Perry, and P. G. Strutton, "Observations of pigment and particle distributions in the western North Atlantic from an autonomous float and ocean color satellite," *Limnol. Oceanogr.* **53**, 2112–2122 (2008).
29. A. Tengberg, J. Hovdenes, J. H. Andersson, O. Brocandel, R. Diaz, D. Hebert, T. Arnerich, C. Huber, A. Kortzinger, A. Khripounoff, F. Rey, C. Ronning, J. Schimanski, S. Sommer, and A. Stangelmayer, "Evaluation of a lifetime-based optode to measure oxygen in aquatic systems," *Limnol. Oceanogr. Methods* **4**, 7–17 (2006).
30. Aanderaa Data Instruments, "TD 218 Operating manual: oxygen optode 3830, 3835, 3930, 3975, 4130, 4175," 78pp (2007).
31. M. S. Twardowski, and W. E. T. Labs, Inc., Department of Research, 165 Dean Knauss Dr., Narragansett, RI, 02882 (personal communication, 2008).
32. H. Buiteveld, J. H. M. Hakvoort, and M. Donze, "Optical properties of pure water," *Proc. SPIE* **2258**, 174 (1994) (doi:10.1117/12.190060).
33. A. Morel, "Optical properties of pure water and pure seawater," in *Optical Aspects of Oceanography*, N. G. Jerlov and E. Steeman Nielsen, eds., (Academic 1974), pp. 1–24.
34. M. S. Twardowski, H. Claustre, S. A. Freeman, D. Stramski, and Y. Huot, "Optical backscattering properties of the "clearest" natural waters," *Biogeosciences* **4**, 1041–1058 (2007).
35. S. W. Bailey, and P. J. Werdell, "A multi-sensor approach for the on-orbit validation of ocean color satellite data products," *Remote Sens. Environ.* **102**(1-2), 12–23 (2006).
36. M. J. Perry, B. S. Sackmann, C. C. Eriksen, and C. M. Lee, "Seaglider observations of blooms and subsurface chlorophyll maxima off the Washington coast, USA," *Limnol. Oceanogr.* **53**, 2169–2179 (2008).

37. B. S. Sackmann, M. J. Perry, and C. C. Eriksen, "Seaglider observations of variability in daytime fluorescence quenching of chlorophyll-*a* in Northeastern Pacific coastal waters," *Biogeosciences Discuss.* **5**, 2839–2865 (2008).
 38. R. Schlitzer, Ocean Data View, <http://odv.awi.de>.
 39. D. Stramski, and D. A. Kiefer, "Light scattering by microorganisms in the open ocean," *Prog. Oceanogr.* **28**(4), 343–383 (1991).
 40. O. Ulloa, S. Sathyendranath, T. Platt, and R. A. Quiñones, "Light scattering by marine heterotrophic bacteria," *J. Geophys. Res.* **97**(C6), 9619–9629 (1992).
-

1. Introduction

Despite their small volume (1% of the global ocean [1]), oxygen minimum zones (OMZ) contribute to about one-third of the oceanic nitrogen loss via denitrification [2]. The distribution of oxygen in these areas is of particular interest because the oxygen concentration will define where aerobic and anaerobic processes take place. Although consensus on a strict oxygen concentration threshold for OMZs has not been reached [3], we concur with an increasingly common upper limit of 20 μM (0.5 ml l^{-1}) dissolved oxygen concentration as a boundary for OMZs [4,5,1]. To date little is known about the dynamics of oxygen minimum zones as a whole, including variability in horizontal extent, vertical thickness, and timing and persistence of intrusions of oxygen-deficient water into the euphotic zone. The world's largest oxygen minimum zone stretches from the eastern subtropical North Pacific (ESTNP) to the eastern South Pacific (ESP) [6,1,7]. Here we focus on the eastern South Pacific oxygen minimum zone, which is a permanent hydrographic feature located directly off the coasts of northern Chile and Peru. It reaches from coastal waters to thousands of kilometers offshore, and can extend from the near surface to depths greater than 700 meters. It is maintained by a combination of low oxygen source waters (Equatorial Subsurface Water, ESSW) and high coastal productivity with subsequent bacterial respiration [3,8].

In addition to chlorophyll *a* (Chl *a*) fluorescence maxima in surface waters, subsurface Chl *a* fluorescence maxima have also been observed within the suboxic waters of the ESP OMZ [9–11]. These features are due to the presence of cyanobacteria, particularly *Prochlorococcus*, at these depths [12,13]. However, little work has been done to characterize the response of the microbial community to forcing from changes in oxygen concentration. Below the photic zone, a distinct and diverse bacterial community thrives in the low oxygen waters of the ESP OMZ [14], including denitrifying [15] and anammox bacteria [12]. These subsurface microbial communities were first observed as intermediate depth nepheloid layers in ship-based profiles of beam attenuation [16–23]. In order to understand the environmental controls on microbial abundance and processes in OMZ, methods for *in situ* sampling and long term monitoring need to be developed and applied in these regions. It is critical that physical, chemical, and biological parameters be sampled at time and space scales that are relevant to both microbial community processes and the physical processes that regulate them. Optical sensors are now being deployed on autonomous platforms that enable researchers to collect biologically relevant data (proxies for phytoplankton abundance and distribution) on times-scales of several days to weeks, months and even years, and on spatial scales of tens to thousands of kilometers [24,25]. Measurements on these scales, taken in combination with hydrographic and chemical (oxygen) measurements, facilitate interpretation of biological data within the context of a dynamic physical environment (*e.g.* short-term wind-driven mixing events, seasonal changes upwelling strength, etc.). Chl *a* fluorescence is the bio-optical parameter most often used as a proxy for Chl *a* concentration, which is itself a proxy for phytoplankton biomass. Backscattering has recently been recognized as another valuable bio-optical parameter because it can be used as a proxy for the distribution and abundance of the bulk particle population [*cf.* 26].

Meso- and large-scale features like the oxygen minimum zone off the coasts of northern Chile and Peru are well suited for monitoring with autonomous platforms. Recent work has shown that autonomous profilers and their complement of sensors can produce robust data for

longer than three years [27,28]. Boss *et al.* [26,28] have also shown that newly developed scattering sensors amenable to autonomous platforms provide useful information about the bulk properties of suspended marine particles. We used Apex floats (Autonomous Profiler Explorer; Webb Research Corporation) to investigate the relationship between the depth of the oxycline, thickness of the oxygen minimum zone, and distributions of the particle assemblage within the OMZ. We quantify the incidence of subsurface chlorophyll and scattering maxima that occur within the anoxic and suboxic waters of the OMZ, and present hypotheses regarding the origin of these signals. To our knowledge, these are the first-ever published autonomous observations to describe the persistent, elevated scattering signals within low oxygen waters.

2. Methods

Two Apex floats (as part of a larger experiment, see <http://omz.udec.cl>) were deployed on 27 March 2008 at 71.6° W, 20.2° S. See Fig. 1 for float trajectories. Each float was equipped with a Sea-Bird SBE 41 CTD, an Aanderaa Optode 3830 for measuring oxygen concentration, and a WET Labs ECO FL-NTU to measure chlorophyll fluorescence and volume scattering at centroid angle 139° and wavelength 700 nm. The floats were programmed to surface at night-time every three days and to collect data on the upcast at 41 predetermined depths. To minimize the effect of large, rare particles on the optical data, the ECO FL-NTU sensors internally averaged 30 samples before reporting a single mean value at each depth bin. Here we analyze data from the floats from 27 March to 16 December 2008. Instruments were checked for drift by examining raw data in deep water (750-1000 m) over time. We examined data over this wide depth range to increase our sample size. The sampling resolution was coarse in deep water, one sample every 50 meters, but the signals were coherent across these depths, which facilitated using them as a whole for drift analysis. No drift was observed (data not shown). We also use this depth range as a “deep water reference” in future calculations for the same reasons.

The Aanderaa Oxygen Optode 3830 operates on the principle of dynamic luminescence quenching [29 and references therein]. Briefly, some materials (luminophores) have a predictable fluorescence response when stimulated with light at a given wavelength. In the case of the Aanderaa Optode sensors, the luminophore is platinum porphyrine, and when excited by blue-green light (505 nm) it emits red photons. There are three characteristics of dynamic luminescence that can be measured: the magnitude, decay lifetime (how long it takes the material to return to a non-luminescent state), and phase shift (the time lag between light excitation and fluorescence emission). In the presence of oxygen, the luminophore molecules have a shorter decay time (oxygen quenches the response), which alters the phase shift of the emitted light. The relationship between the phase shift and oxygen concentration is well known for platinum porphyrine. The Optode sensor emits a blue-green light modulated at 5 kHz, and directly measures the phase shift with digital signal processing electronics. The sensor uses a built in thermistor to estimate the temperature-dependent oxygen concentration. Post-processing corrections include salinity and depth compensations [30]. The manufacturer stated accuracy and resolution of the Oxygen Optode 3830 are < 8 μM and < 1 μM respectively, with a settling time of < 25 seconds [30].

The following procedure was used to convert the ECO FL-NTU turbidity, τ , to the particulate backscattering coefficient, $b_{bp}(700\text{ nm})$ [31]. We first estimated backscattering due to pure seawater at 700 nm using temperature (T) and salinity (S) from *in situ* data in deep water ($b_{bsw}(T,S,700\text{ nm})$; 750 to 1000 meters) and theoretical equations for pure seawater scattering [32–34]. We then estimated total backscattering in deep water, b_{bt}^{deep} by multiplying b_{bsw} by 1.11 (we assumed that 90% of the backscattering signal is pure seawater, based on previous measurements in deep water in the South Pacific by *Twardowski et al.* [34], off Hawaii and in the Ligurian Sea [31]). Using raw instrument counts and manufacturer calibration values for dark counts and the scaling factor, we estimated turbidity in deep water,

τ^{deep} . Then, we used b_{bt}^{deep} and τ^{deep} to obtain a conversion factor (CF) where $CF = b_{bt}^{deep} / \tau^{deep}$ [$m^{-1} NTU^{-1}$]. The CF was then used to compute the total backscattering coefficient, b_{bt} , for the whole water column where $b_{bt} = \tau * CF$. Finally, we obtained b_{bp} by subtracting the value for b_{bsw} from the first step from b_{bt} .

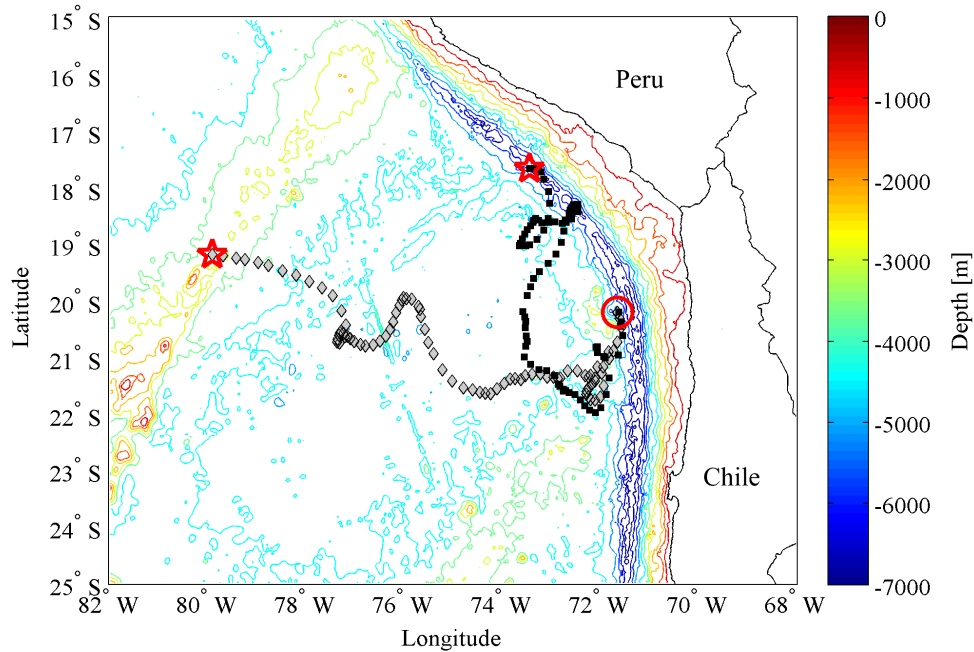


Fig. 1. Float trajectories for two Apex floats over time. Color bar indicates depth of bathymetry contours in meters. The grey diamonds are float 62164; the black squares are float 62166. For both floats the red circle indicates the launch location on 27 March 2008, and the red star indicates the location of the float on 18 December 2008. The time between each surface location is three days.

The conductivity sensor on float 62164 failed after 53 profiles. Following this failure, we used the average salinity from the first 50 profiles from 750 to 1000 meters, which was 34.487, with a standard deviation of 0.0083. In a sensitivity analysis on the effect of salinity on our estimate of the backscattering coefficient, we found that over the maximum range of salinities observed in our study area (34 – 35.5), variability in the estimated backscattering coefficient was approximately 1%. Although there is admittedly $\pm 5\%$ uncertainty in the assumption of 90% seawater contribution for deep water, an advantage of this method is that backscattering magnitudes were significantly higher in the overlying water column. Propagated accuracies associated with this assumption were thus less than 1% from the surface to the base of the oxygen minimum zone.

Given the fact that the conversion from turbidity to backscattering units is performed after the instrument factory calibrations have been applied, one would expect the conversion factors for both floats to agree. Unfortunately, we found that the mean and median CFs were statistically different (t-test and Wilcoxon rank sum test respectively). The mean, median and standard deviation for CFs from float 62164 were 0.0094, 0.0095, and 4.59×10^{-4} respectively. The mean, median and standard deviation for CFs from float 62166 were 0.0076, 0.0077, and 5.65×10^{-4} respectively. The most likely explanation for the discrepancy is uncertainty in the factory calibration, specifically the dark counts. Boss et al. [28] performed multiple instrument calibrations on their LSS turbidity sensor (WET Labs) immediately prior to deployment and found that the dark counts differed from the manufacturer calibration by more than eight counts in the best case, and by more than 17 counts in the worst case. Changes

between eight and seventeen dark counts in our calibrations would result in backscattering magnitudes that differ between 6 and 65 percent compared to the values produced using the factory dark counts, depending on whether the dark counts shifted up or downward and by how much.

We were unable to independently calibrate our ECO FL-NTU sensors prior to deployment, so the absolute magnitude of our turbidity (and hence backscattering) estimates may be inaccurate. However, in the absence of instrument drift, information gathered from relative changes in particulate backscattering intensity is still extremely valuable. Under the assumption that the conversion factor is constant over the entire water column, any relative error associated with the CF would be determined by the constant ratio of our estimated CF to the 'actual' CF (if we could measure dark counts perfectly). At high signals, as in the surface waters and within the OMZ, this error becomes small and relative changes in the backscattering signal should be very accurate (*i.e.*, the relative error is small). While the true magnitude of backscattering is not well resolved in our data, variability in the total particle load and characteristics of the bulk particle population are reflected in the variation of the backscattering signal over time and space. In this work we emphasize the conclusions that can be drawn from these relative changes in backscattering, and leave more accurate determinations of the absolute magnitude of backscattering in oxygen minimum zones for another occasion.

As with the scattering channel on the ECO FL-NTU sensors, we were unable to collect dark counts or scaling factors for the chlorophyll fluorescence channels prior to the deployment of the floats. Vicarious satellite calibrations for autonomous fluorescence sensors have been utilized with some success elsewhere [27,28]. However, given that the uncertainty of satellite derived chlorophyll estimates is 33% [global average, median percent difference between SeaWiFS and *in situ* data; [35], we considered this vicarious correction method as a last resort, only to be used to correct for substantial sensor drift, had there been any. The best possible method of post-deployment calibration would have been to use discrete estimates of Chl *a* from nearby ship-based samples. Unfortunately, we had no such data available. Another method for *in situ* sensor correction is to estimate a "background" signal with measurements in deep water, and then remove this background from all data after the manufacturer-supplied calibrations have been applied [36,37]. This method reduces the chlorophyll signal to zero in clear water and can account for sensor drift over time. While this approach is logical, we did not observe any drift in the deep-water fluorescence counts (slopes of linear fits to the data over time were not significantly different than zero), and we did not feel it was necessary to scale our data in this manner. As such, we present the data with the factory calibrations applied, and offer the caveat that any offset in calibration coefficients that may have occurred between the factory calibration and deployment would be reflected in the data set.

In order to quantify the occurrence of subsurface backscattering maxima in our profiles, we set a few criteria. We excluded data shallower than 50 meters, and set a lower threshold for particulate backscattering at 0.0001 m^{-1} . We also required at least two continuous data points above the threshold to qualify a subsurface signal as a genuine "maximum". While more data points would be desirable, it must be recognized that measurements were taken between ten and fifty meters apart in the water column, and that the internal averaging of the FL-NTU sensor over thirty seconds strengthens our confidence that observed signals were indeed the result of a higher particle concentration and were not due to sampling of a rare, single large particle. Secondary Chl *a* maxima in subsurface waters were far easier to qualitatively identify than backscattering features. Because the depth range of the Chl *a* signal was restricted to the photic zone, we removed the restriction of two continuous data points, and set no minimum threshold.

3. Results

We analyzed data from a total of 173 profiles of temperature, salinity, oxygen concentration, Chl *a* concentration, and particulate backscattering at 700 nm in the ESP OMZ. Time-series data (plotted as distance along the track line) of hydrographic and optical properties from float 62164 are shown in Fig. 2, and for float 62166 in Fig. 3 [Ocean Data View; 38]. The contour plots of the backscattering coefficient show a persistent intermediate-depth particle maximum that consistently extended from the oxycline (dissolved oxygen reduction of up to 21 $\mu\text{M m}^{-1}$) down to the base of the OMZ (between 350 and 450 meters deep; Figs. 2, 3 and 4). A strong backscattering signal associated with the oxygen minimum zone was observed in 82.7% of all profiles (both floats combined; Table 1). The depth range of the particle maximum appears to be constrained by the limits of the oxygen minimum zone in most cases (white contour lines in Figs. 2 and 3). This phenomenon is especially evident in Fig. 3, where elevated levels of backscattering at intermediate depths were restricted to suboxic waters ($< 4.5 \mu\text{M}$ or 0.1 ml l^{-1}), and were observed throughout the drifter track except where there were apparent intrusions of water with slightly higher oxygen concentrations.

Table 1. Enumeration of fluorescence and particulate backscattering signals in the eastern South Pacific oxygen minimum zone.

| Float number | 62164 | % | 62166 | % | Both | % |
|--|-------|------------|-------|------------|------|------------|
| Total number of profiles | 89 | <i>n/a</i> | 84 | <i>n/a</i> | 173 | <i>n/a</i> |
| Total w/elevated b_{bp} in OMZ | 64 | 71.9 | 79 | 94.0 | 143 | 82.7 |
| Total w/elevated Chl- <i>a</i> in OMZ | 18 | 20.2 | 31 | 36.9 | 49 | 28.3 |
| Profiles w/elevated b_{bp} only | 47 | 52.8 | 49 | 58.3 | 96 | 55.5 |
| Profiles w/elevated Chl- <i>a</i> only | 1 | 1.1 | 1 | 1.2 | 2 | 1.2 |
| Profiles w/elevated b_{bp} & Chl- <i>a</i> | 17 | 19.1 | 30 | 35.7 | 47 | 27.2 |

Another notable phenomenon found in our observations was a subsurface Chl *a* maximum in suboxic waters. We observed this subsurface Chl *a* signal within suboxic waters in 28.3% of all profiles (Table 1). These subsurface features were nearly always observed when the oxycline was shallower than approximately 100 meters in depth and displayed a lower magnitude than Chl *a* concentrations in oxygen-containing surface waters (e.g. Figure 4A). For example, during the first ~200 kilometers of the track line for float 62164, the float was close to shore where the oxycline was relatively shallow and subsurface Chl *a* signals were evident (Fig. 2). When the float drifted offshore the depth of the oxycline deepened, resulting in an unsuitable light environment for photosynthetic organisms within the OMZ. Following this change, there was only one observation of a subsurface Chl *a* maximum in the remainder of the data set for this float. Float 62166 remained closer to shore than float 62164, and the shallower depth of the oxycline over its trajectory resulted in nearly twice as many observations of a secondary Chl *a* maximum in low oxygen waters, 31 and 18 for the two floats respectively (Table 1). Chl *a* peaks detected within the OMZ rarely extended below 125 meters, and were nearly always coincident with an increase in the backscattering signal.

4. Discussion

Intermediate depth particle maxima associated with oxygen minimum zones have been observed in several ship-based sampling studies dating back to the late 1970's [16–23]. *Pak et al.* [1980] observed particle maxima using light transmission measurements at several locations off the coast of Peru. The signals were located in low oxygen waters, but the authors could not identify the nature of the particles or their source. *Pak et al.* [1980] ruled out

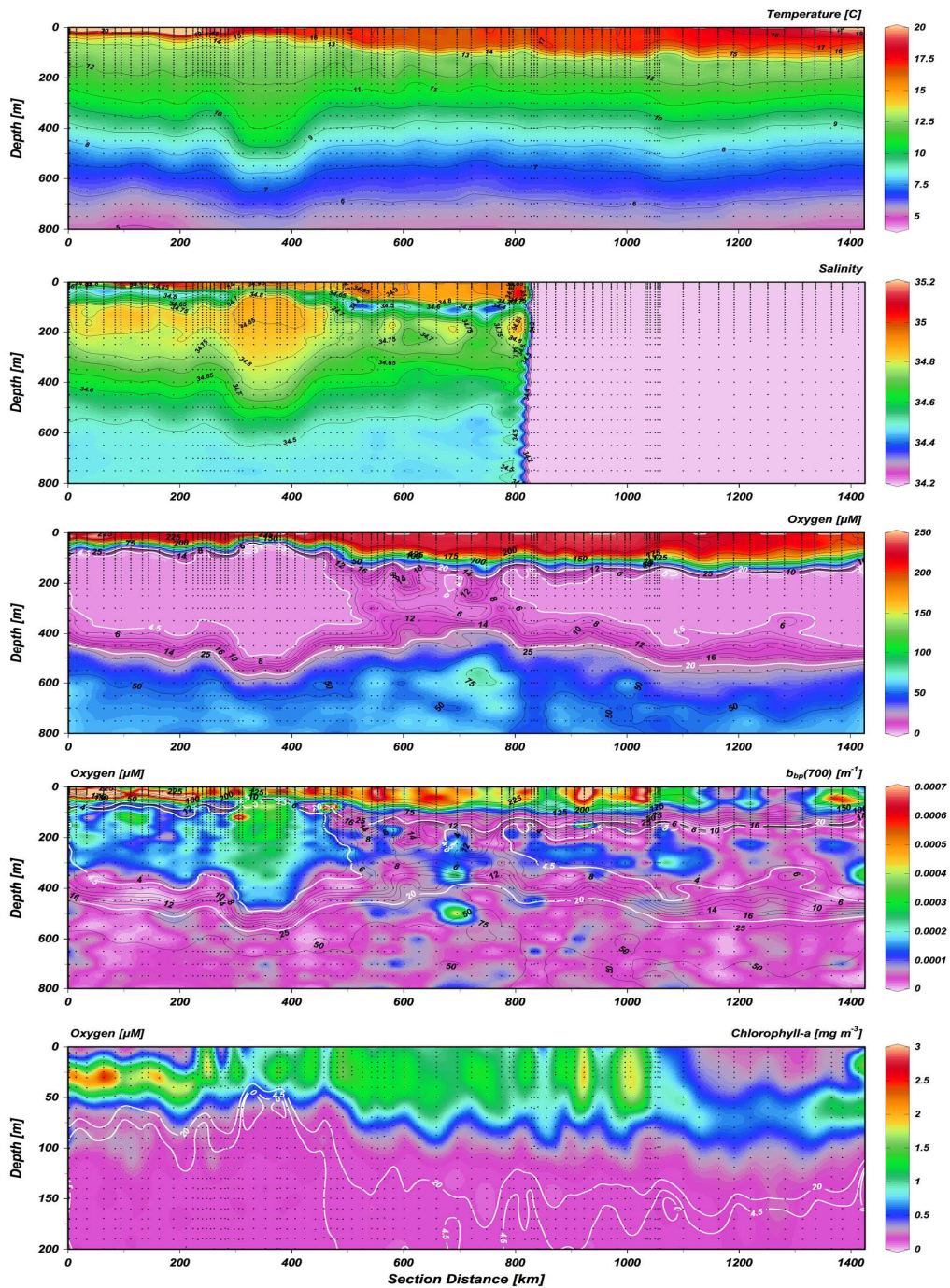


Fig. 2. Progression of temperature, salinity, oxygen, particulate backscattering at 700 nm, and Chl *a* concentration over time/distance and depth in the oxygen minimum zone off of Chile. Data are from float 62164. Sample locations are shown as black dots. All plots show the depth range from the surface to 800 meters, except Chl *a*, which shows data from the surface to 200 meters only. White contour lines show the oxygen concentration at 4.5 and 20 μM . Black contour lines on the panel showing the backscattering data represent the oxygen concentration in μM . The failure of the conductivity sensor is evident at approximately 800 km into the float trajectory. Sections produced using Ocean Data View software [Schlitzer, 2009].

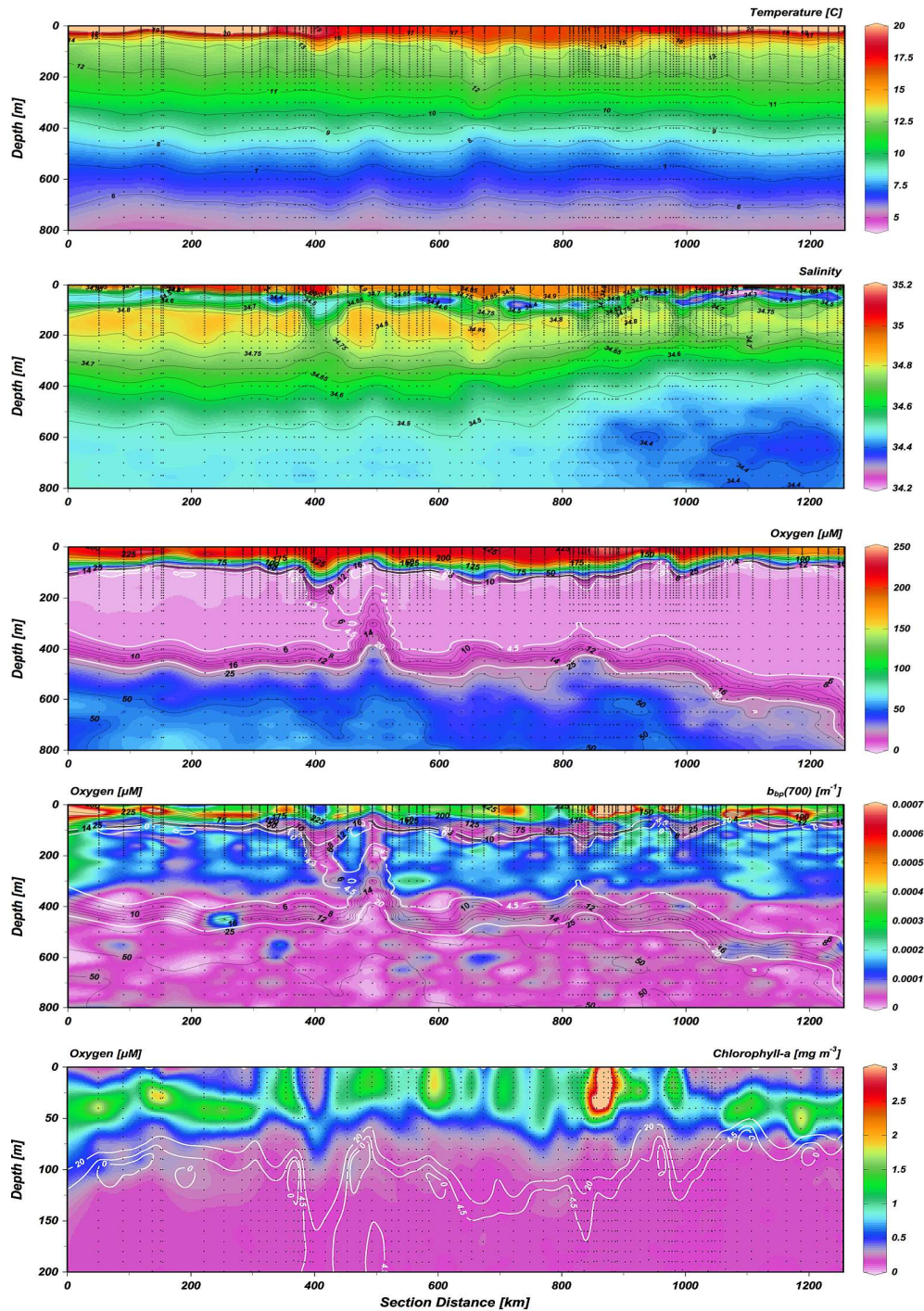


Fig. 3. Progression of temperature, salinity, oxygen, particulate backscattering at 700 nm, and Chl *a* concentration over time/distance and depth in the oxygen minimum zone off of Chile. Data are from float 62166. Sample locations are shown as black dots. All plots show the depth range from the surface to 800 meters, except Chl *a*, which shows data from the surface to 200 meters only. White contour lines show the oxygen concentration at 4.5 and 20 μM . Black contour lines on the panel showing the backscattering data represent the oxygen concentration in μM . Sections produced using Ocean Data View software [Schlitzer, 2009].

offshore transport of bottom nepheloid layers as a formation mechanism for consistent particle maxima observed at 400 meters depth, but did not suggest an alternative hypothesis for their origin. *Kullenberg* [1981] observed subsurface particle scattering maxima in several profiles collected off the coast of Peru (at many of the same stations sampled by *Pak et al.* [1980]), but he did not firmly link the signal with a potential source. Current meter data did not support the mechanism of offshore transport of particles, so *Kullenberg* [1981] hypothesized that alongshore advection and/or particle sinking might explain the signals. While *Kullenberg* [1981] did associate the scattering maxima with coincident nitrite maxima, he did not go so far as to propose that the scattering could be the result of bacterial production *in situ*.

Garfield et al. [1983] were the first to make a strong case for *in situ* bacterial production as a mechanism for the persistence of a subsurface particle maximum in oxygen minimum zones. Based on profiles of light transmission, dissolved oxygen, nutrients (including nitrite and nitrate), and electron transport system activity in the oxygen minimum zone off of Mexico, *Garfield et al.* [1983] concluded that denitrifying and ammonium oxidizing bacteria were likely an important component of the particle population that generated the intermediate depth particle maximum in their observations. The authors also found that a particle maximum at 200 meters depth in the oxygen minimum zone was associated with specific water mass characteristics. The water mass had salinity around 34.8 and temperature around 13 °C, which corresponded to a sigma-*t* value of 26.4. *Garfield et al.* [1983] argued that particle association with a water mass, rather than near a pycnocline, was indicative of advective or *in situ* production processes rather than particle sinking.

Previous observations of particle maxima in oxygen minimum zones set a solid foundation for our work. However, previous studies lacked sustained observations of these features that would enable characterization of the spatial and temporal dynamics of particles in OMZs. This is where our work makes an important contribution. Nine months of data from two floats, which surfaced every three days, provided semi-continuous, near real-time observations of hydrographic and bio-optical parameters in the ESP OMZ. Our results show that elevated backscattering signals occur in suboxic waters in over 80% of profiles that covered a combined drifter track of over 2,600 kilometers (both floats combined). The drifter that remained closer to shore, 62166, captured subsurface scattering signals in the OMZ in 94% of profiles, compared with only 72% of profiles for float 62164. We attribute this difference to the greater persistence of a low-oxygen environment in the nearshore observations (compare oxygen sections in Figs. 2 and 3), which should maintain a more stable habitat for microbes with anaerobic metabolisms that appear to dominate in the OMZ [14]. Disruptions in the low-oxygen environment, e.g. apparent intrusions of water with higher oxygen concentration, were accompanied by decreased backscattering signals from both floats. The response of the particle population to this kind of physical forcing would be very difficult to observe with ship-based measurements.

Although our data were collected in a different area (South rather than North eastern tropical Pacific), TS-diagrams produced from data collected with the Apex floats strongly resembled those reported by *Garfield et al.* [1983] (Fig. 5). We found that low oxygen waters were generally associated with a maximum salinity between 34.5 and 34.9, and temperatures between 8 and 13 °C. These data corresponded to sigma-*t* values between 26 and 27, centered around 26.4 (Fig. 5). TS data from float 62164 displayed less variability than data from float 62166. We attribute this to the reduced size of the data set resulting from the conductivity sensor failure, not to differences in the hydrography of the OMZ in the areas of the float trajectories. Figure 5 also shows that the elevated backscattering signals from the subsurface particle maximum were associated with the same water mass as the low oxygen waters. Given these results, we concur with the conclusions reached in *Garfield et al.* [1983], and believe that the particles that dominated the backscattering signal in our research area were likely produced via *in situ* production rather than advective processes.

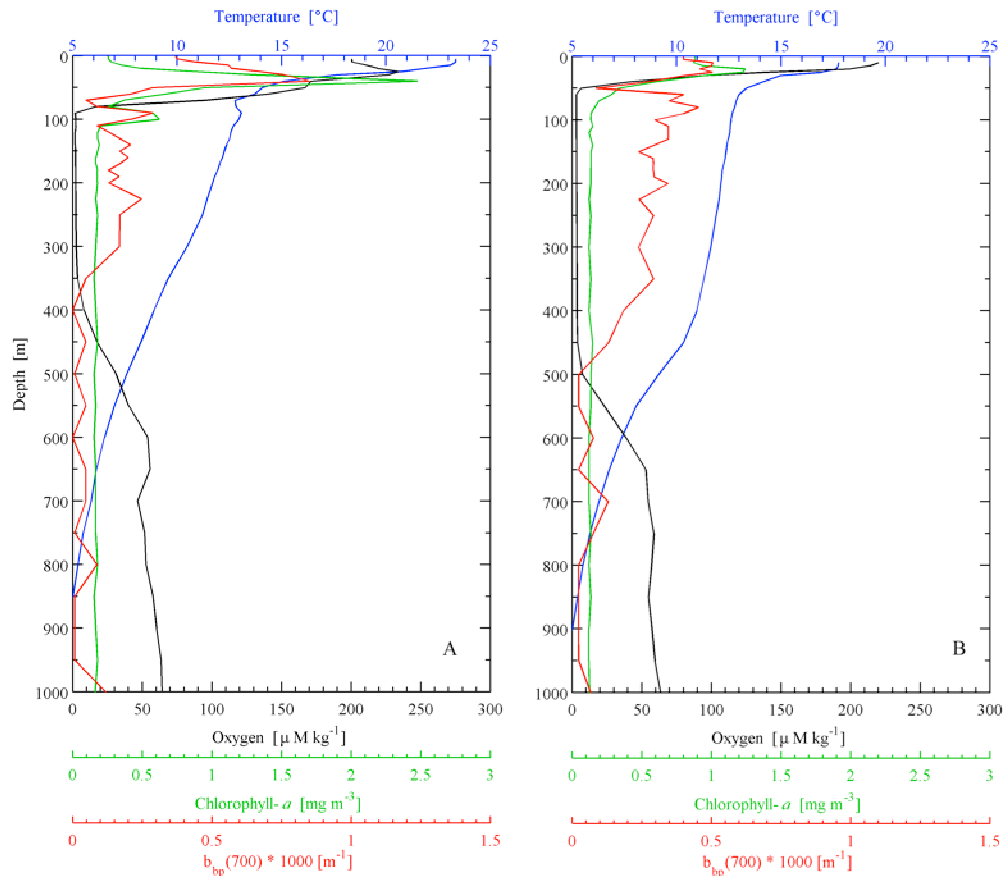


Fig. 4. Representative profiles from float 62164 of temperature, oxygen, Chl *a*, and backscattering from the oxygen minimum zone off of Chile. A) Subsurface Chl *a* peak and elevated backscattering signals are evident in hypoxic waters. B) Only a subsurface backscattering signal is present within the OMZ.

While we have no direct evidence that marine microbes generated the enhanced backscattering signals that we observed at intermediate depths, we hypothesize that non-photosynthetic marine microbes represented a stable and significant portion of the total particle population within the ESP OMZ. *Spinrad et al.* [1989] and *Naqvi et al.* [1993] showed a strong relationship between bacterial counts and the beam attenuation coefficient in the coastal waters off of Peru and the northwest Indian Ocean respectively. *Spinrad et al.* [1989] did not measure the oxygen concentration, but the presence of strong nitrite maxima and the location of their study area support the assumption that their observations were within an OMZ. *Naqvi et al.* [1993] definitively linked denitrification, beam attenuation, and bacterial abundance in an intermediate depth nepheloid layer in the Arabian Sea OMZ, and suggested that this phenomenon was likely to occur globally wherever denitrifying conditions exist (*i.e.* the presence of increased particle load in oxygen minimum zones due to enhanced microbial activity). Though we measured backscattering rather than the attenuation coefficient, beam attenuation and backscattering both vary to a first order with particle concentration. Given the high backscattering efficiency of small particles [39], we would expect to find a relationship similar to that observed by *Naqvi et al.* [1993] between the density of microbes and the backscattering coefficient in our data [*cf.* 40].

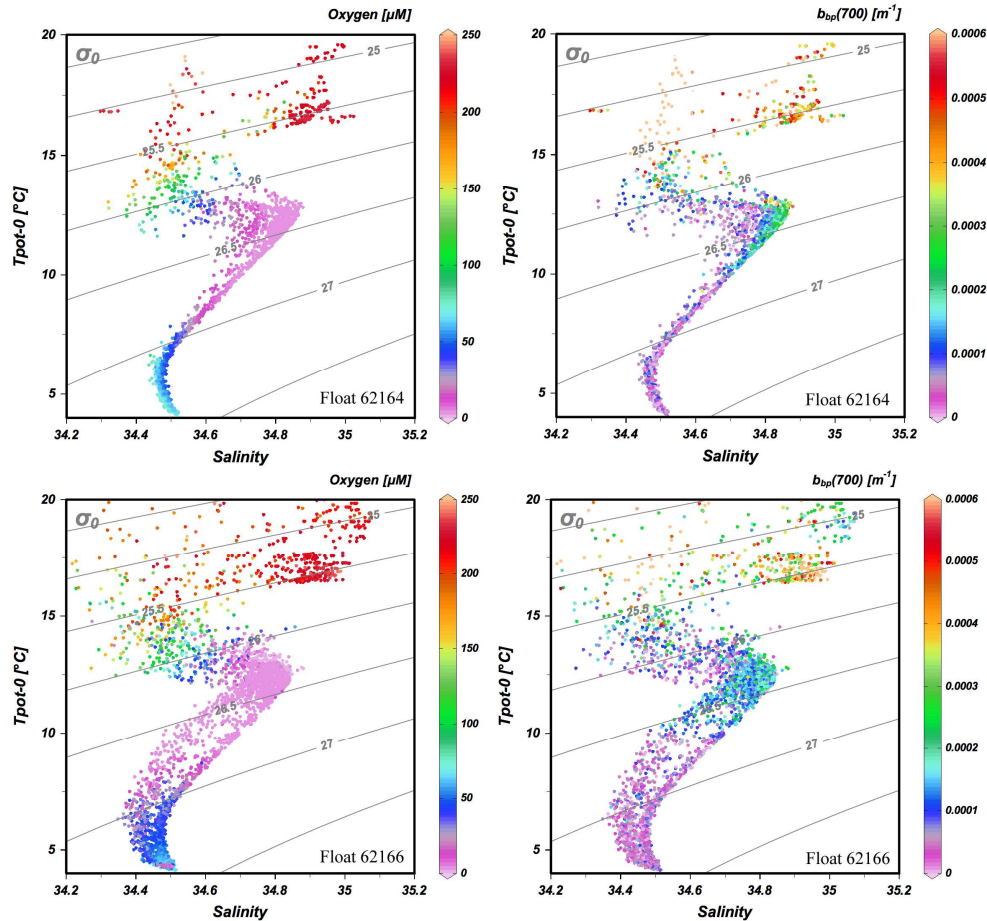


Fig. 5. Potential temperature/salinity (TS) diagrams showing data from two Apex profiling floats located in the eastern south Pacific oxygen minimum zone. The top row is all data collected from float 62164 before the conductivity sensor failure, and the bottom row is all data collected from float 62166. The color of the TS-diagrams on the left show the oxygen concentration, and on the right the colors represent the magnitude of the particulate backscattering coefficient at 700 nm. Isopycnals are shown on all TS-diagrams.

The apparent restriction of the intermediate-depth backscattering signal to waters with oxygen concentrations of less than $4.5 \mu\text{M}$ (0.1 ml l^{-1}) also implies that active microbial metabolic processes were at least partially responsible for the maintenance of the backscattering feature [22,23]. The $4.5 \mu\text{M}$ threshold marks an important metabolic shift from oxygen-based respiration to denitrification, and reduced oxygen levels would likely inhibit the presence of heterotrophic grazers [23]. If the signal were solely derived from transport of inorganic particles within the oxygen minimum zone, we would have expected to observe scattering signals throughout low oxygen waters (up to $20 \mu\text{M}$). However, we found that the depth range of the backscattering signal did not extend through the whole oxygen minimum zone (to 500 meters), but was usually confined to the lower limit of suboxic waters only (300 to 400 meters; see Figs. 2, 3 and 4).

Lastly, observations of increased backscattering at these depths relative to areas without an OMZ provide evidence of augmented microbial biomass in oxygen free environments. Our preliminary results indicate that optical methods could yield important information about spatio-temporal distributions of microbial assemblages in the ESP OMZ at relevant scales.

5. Conclusions

The fascinating, diverse community of marine microbes within the oxygen minimum zone likely plays an important role in the marine nitrogen cycle in these regions, but our understanding of the spatial and temporal dynamics of these microbes remains limited. Historically, *in situ* bio-optical methods in oceanography rarely focused on non-Chl *a* containing bacteria and archaea, but our results indicate that the addition of a backscattering sensor on autonomous floats can provide important insights into microbial community dynamics, *i.e.* in response to physical (T, S) and chemical (O₂) forcing. We observed elevated backscattering levels throughout the ESP OMZ in over 82% of all profiles. These signals were evident over several months and hundreds of kilometers of drifter observations. For float 62166, particulate backscattering signals in the OMZ were continuous over the entire drifter track, with the exception of short perturbations associated with higher oxygen waters. Data from float 62164, which drifted offshore, demonstrated more episodic backscattering signals within the OMZ. The subsurface backscattering signals from both floats were nearly always constrained by the upper and lower depth limits of the 4.5 μM dissolved oxygen concentration. We hypothesize that these signals were due to high abundances of non-photosynthetic microbes that thrive in an oxygen-deficient environment. We cannot rule out the possibility that some portion of the signal was associated with the advection of particles. The fact that the particles were associated with a specific water mass and that the signals were more consistent in the float that remained closer to shore both support the possibility of an advective particle source, regardless of whether the particles were lithogenic or biological in origin. We also observed significant peaks in Chl *a* fluorescence within suboxic waters when the OMZ penetrated the euphotic zone (28% of profiles).

This work contains the first published autonomous observations of enhanced particle concentrations associated with oxygen minimum zones using optical methods, and confirms the utility of autonomous tools in monitoring physical and particle/microbial dynamics in these areas. Our future efforts will augment the float measurements with ship-based profiles of particulate backscattering, Chl *a* fluorescence, and hyperspectral upwelling and downwelling plane irradiance. We are also monitoring the spatio-temporal variability in oxygen and the intermediate scattering layer on finer scales in the ESP OMZ with autonomous gliders. The end goal is to elucidate the origin of the particle maxima (local vs. advective sources), characterize the nature of the particle population (living and non-living biological vs. lithogenic material), and describe how physical and chemical forcings regulate them.

Acknowledgements

The authors thank Oscar Pizarro (UdeC) for his valuable contribution to the experiment design and floats deployment, and Dana Swift for assistance in accessing float data. The data processing method for the ECO FL-NTU sensor was modified and improved during valuable discussions with Mike Twardowski, Emmanuel Boss, and Francesco Nencioli. The authors thank an anonymous reviewer for helpful comments and suggestions. This work was supported by the Agouron Institute (Grant AI-MME1.05).